ALEPH 94-010
PHYSIC 94-009
A. Halley and P. Colrain
27.01.1994

# Measuring $A_{FB}^{b\bar{b}}$ from the Charge Asymmetry in Lifetime-Tagged Hadronic Events

Andrew Halley (Max-Planck-Institut für Physik, München)
Paul Colrain (The University of Glasgow, Scotland)

Thursday the $27^{th}$ of January, 1994

**Abstract**

A measurement of $A_{FB}^{b\bar{b}}$ using the lifetime-tag and the hemisphere-charge method is presented. The mean charge asymmetry in an 88%-pure $b$ sample of the 1991 & 1992 data is measured to be 104 ($\pm 11_{stat.} \pm 2_{syst.}$) $\times 10^{-4}$. Using the lifetime-tag measurement in data to calibrate the $b$-quark hemisphere-charge, the asymmetry is determined to be :

$$A_{FB}^{b\bar{b}} = 10.65\ (\pm 1.09_{stat.} \pm 0.42_{syst.})\,\%$$

The effective electroweak mixing angle is extracted, neglecting explicit QCD corrections but taking into account the thrust axis resolution. The measured value close to the $Z$ peak is :

$$sin^2\theta_w^{eff} = 0.2303\ (\pm 0.0020_{stat.} \pm 0.0008_{syst.})$$

The techniques employed in the analysis are explained in detail, together with the sources of systematic errors and prospects for future measurements.

## 1 Motivation

Measurements of quark forward-backward asymmetries allow one of the most precise determinations of the electroweak mixing angle, $sin^2\theta_w^{eff}$[1] . As the volume of LEP data grows, it is important to isolate the most statistically significant and least systematically limited channels so as to make competitive measurements. The statistical significance of quark channel measurements can be seen from the Standard Model framework of on-resonance asymmetries, which may be written as :

$$A_{FB}^{f\bar{f}} \approx \frac{3}{4}\,\mathcal{A}_e\,\mathcal{A}_f \quad \text{for a flavour of fermion } f, \tag{1}$$

where :

$$\mathcal{A}_e = \frac{g_L^2 - g_R^2}{g_L^2 + g_R^2} = \frac{2(1 - 4\,|Q_f|\,sin^2\theta_w^{eff})}{(1 + (1 - 4\,|Q_f|\,sin^2\theta_w^{eff})^2)}. \tag{2}$$

The advantage of quark measurements lies in the fact that $\mathcal{A}_e$ is very sensitive to $sin^2\theta_w^{eff}$ whereas $\mathcal{A}_{d,s,b}$ are large, leading to large asymmetries and cross-sections. The $b$ quark is further favoured by having a large tagging efficiency as a result of its large mass and long lifetime.

Previous quark asymmetry measurements have either used the hemisphere-charge method *without* flavour tagging [2, 3, 4] or high $(p, p_t)$ leptons to tag both the charge and presence of $b$ quarks [5, 6]. Both methods rely on Monte Carlo models to determine the contributions from the charge asymmetries of various quark flavours to the measured asymmetry. This, and $B^0\bar{B}^0$ mixing, represent the dominant systematic uncertainties.

The analysis presented here makes use of the *double-tag* techniques of the lifetime-tag [7] and hemisphere-charge measurements from data [11, 12] to measure the asymmetry and extract $sin^2\theta_w^{eff}$ whilst constraining systematic uncertainties from the use of Monte Carlo models.

## 2 Method

$A_{FB}^{b\bar{b}}$ is obtained by measuring the forward-backward asymmetry in a $b\bar{b}$ enriched sample of events. This measurement makes use of two physics algorithms; the lifetime-tagging procedure, QIPBTAG [8], and the hemisphere-charge method explained in [2, 9, 10]. The event selection and application of the tagging algorithm to create a large heavy-flavour sample, is described in Section 3. The electroweak asymmetry is then measured by taking the difference between reconstructed *hemisphere-charges* in the forward and backward ($\pm$Z) detector hemispheres of selected events, namely :

$$\langle Q_{FB} \rangle = \langle Q_F - Q_B \rangle \tag{3}$$

The two hemisphere-charges are calculated using a $p_L$-weighted charge summation[1] running over the charged tracks in an event subject to a weighting power, $\kappa$. The asymmetry in a lifetime-tagged quark sample may be written as :

$$\langle Q_{FB}^{btag} \rangle = \sum_{f=u,d,s,c,b} \delta_f \; C_f \; A_{FB}^{f\bar{f}} \; \mathcal{P}_f \tag{4}$$

where it is useful to define the following quantities :

$\delta_f$ is the mean $\langle Q_{FB} \rangle$ in ALEPH for a quark of type $f$ moving in the *forward* direction[2],

$C_f$ is the acceptance for this flavour of quark, $f$,

$\mathcal{P}_f$ is the purity for quark flavour $f$.

Initially the tagging efficiency and weighted charge summation are optimised so as to maximise the statistical significance of the measurement. This is explained in Section 4 while systematic uncertainties are taken into account later in Section 10. The large selection efficiency of the lifetime-tagging algorithm means that the severe dilution of the primary $b-\bar{b}$ quark charge ($\pm\frac{2}{3}$) from the hemisphere-charge method remains tolerable. The strength of these two algorithms lies in the way in which they are calibrated using the data as far as is possible. This is shown in [7] for the lifetime-tag whilst the two complementary measurements of the $b$ hemisphere-charge are discussed in Section 8.

The extraction of electroweak parameters from the measured asymmetry requires knowledge of the detector's angular acceptance for tagged events. This is dominated by the VDET acceptance for $b$ events and can be parameterised simply in terms of $cos\,\theta_{thrust}$, where $\theta_{thrust}$ is the angle of the thrust-axis relative to the beams. This is outlined in Sections 6 and 7 while the measured asymmetries are summarised in Section 5. An electroweak fit is then performed, using the ZFITTER package to provide radiative corrections to the tree-level quark asymmetries. The fitting procedure is used repeatedly to calculate the statistical and systematic errors of the measurement as described in Section 9. Solving iteratively for the values of $A_{FB}^{b\bar{b}}$ and $sin^2\theta_w^{eff}$ which best fit the data yields the results given in Section 10.

## 3 Event Selection and Lifetime-Tagging

Data are selected primarily using the $q\bar{q}$ hadronic event selection based upon charged tracks (the CLAS 16 algorithm). The 1991 % 1992 data are used for those runs passing the official VDET selection criteria in SCANBOOK. In addition, checks are made upon the relevant (ENFLW relevant) subdetector voltages, including XVDEOK, and finally for DAQ errors. The number of events used and those failing the above selections are summarised in Table 1. The thrust axis[3] is used to

[1] The hemisphere-charge formalism used throughout is that of [2].

[2] The value of $\delta_f$ is actually taken to be the mean of $\delta_f$ and $\delta_{\bar{f}}$ as they are equivalent at the present level of accuracy. This is often referred to as the hemisphere-charge *separation* for this flavour.

| Category | Events |
|---|---|
| *Events read from tape :* | 680,670 |
| *Events without* HCAL *voltage :* | 39 |
| *Events without* ECAL *voltage :* | 1,597 |
| *Events without* ITC *voltage :* | 1,429 |
| *Events without* TPC *voltage :* | 2,908 |
| *Events without* VDET *voltage :* | 3,730 |
| *Events with* DAQ *errors :* | 205 |
| *Events with two few charged tracks :* | 30 |
| *Events having too little charged energy :* | 119 |
| *Events surviving event selection :* | 671,362 |
| *Events without a charged track in each hemisphere :* | 471 |
| *Events outside the* $\cos\theta_{thrust} \leq 0.8$ *acceptance :* | 165,428 |
| *Events with less than two* QIPBTAG *jets :* | 386 |
| *Events with jets outside* QIPBTAG *acceptance :* | 6,492 |
| *Events without a track passing* QIPBTAG *cuts :* | 1,009 |
| *Events available for the asymmetry analysis :* | 505,934 |

Table 1: *Summary of events used and rejected by the event selection cuts described in the text.*

define the angular acceptance. It is calculated using charged and neutral ENFLW objects. For reasons explained in Section 6, events are selected for which $|\cos\theta_{thrust}| \leq 0.8$. The number of events surviving this cut are also listed in Table 1. Applying the lifetime-tagging algorithm introduces some small losses by demanding that at least one track has VDET hits and passes QIPBTAG selection criteria. It also requires that the jets used lie within a very loose angular acceptance of $|\cos\theta| \leq 0.995$. In the events already chosen to pass the $\cos\theta_{thrust} \leq 0.8$ cut these additional criteria have little effect and the tag itself is almost completely efficient.

The tracks used later to define the hemisphere-charges are corrected using the sagitta corrections derived from the collinear muon analysis [14]. These corrections depend on the angle of the track and are due to residual field distortions within the TPC. The statistical uncertainty on the corrections from data are then used as a systematic error.

The $q\bar{q}$ hadronic event selection is known to contain a very small contamination from two-photon and $\tau^+\tau^-$ background events, at a level of 0.3 and 0.2 % respectively. The former are unlikely to contribute an additional asymmetry due to the nature of the physics process involved. The $\tau^+\tau^-$ contribution, whilst non-zero, is supressed by the small value of the $Z$ peak $\tau$ asymmetry and the low selection efficiency and hence may be safely neglected [9].

As $A_{FB}^{b\bar{b}}$ represents a *ratio* of events, the *efficiency* of the tag cancels and it is only the *purity* which is relevant for this analysis. The lifetime-tag provides two *hemisphere tag probabilties* for each event. An increasingly pure $b$ sample is obtained by demanding that *at least one* hemisphere passes a given cut on these hemisphere tag probabilties. It is then useful to define :

$$\begin{aligned} \varepsilon_f^h &= \text{the efficiency to tag a hemisphere of flavour } f, \\ \varepsilon_f^e &= \text{the efficiency to tag an event of flavour } f, \end{aligned} \tag{5}$$

which are related by :

$$\varepsilon_f^e = 2\varepsilon_f^h\left(1 - c_f\varepsilon_f^h\right) + c_f\left(\varepsilon_f^h\right)^2. \tag{6}$$

$c_f$ are the flavour-dependent correlations between the hemispheres, of which only the $b$ term, $c_b$, is of importance. These correlation terms may be related to the $\lambda_f$ of the $\Gamma_{b\bar{b}}$ analysis [7] via

[3] A comparison using the sphericity axis has been performed. No discernible difference or improvement was observed.

the relation :

$$c_f = \lambda_f \frac{1}{\varepsilon_f^h}\left(1 - \varepsilon_f^h\right) + 1 \tag{7}$$

The values for $\varepsilon_f^h$ and $\lambda_f$ are those used[4] in the ALEPH $\Gamma_{b\bar{b}}$ analysis [8]. The purities for different flavours are then calculated using :

$$\mathcal{P}_f = \frac{\varepsilon_f^e}{\varepsilon_{Total}^e} \frac{\Gamma_{f\bar{f}}}{\Gamma_{had}} \tag{8}$$

where $\varepsilon_{Total}^e$ is the overall tagging efficiency for all flavours combined.

The values for $\Gamma_{c\bar{c}}$ and $\Gamma_{b\bar{b}}$ are correlated with the values of $\varepsilon_f^h$ and $\varepsilon_f^e$. The expected Standard Model (SM) values are assumed for light quarks as their significance is small. They are then re-scaled so that the total of the light quark fractions, and $(\Gamma_{c\bar{c}}, \Gamma_{b\bar{b}})$ from [7], is unity. These values are summarised in Table 2. The resulting purities for these tag cuts are shown in Table 3.

| $-log_{10}(cut)$ | $\Gamma_{u\bar{u}}/\Gamma_{had}$ | $\Gamma_{d\bar{d}}/\Gamma_{had}$ | $\Gamma_{s\bar{s}}/\Gamma_{had}$ | $\Gamma_{c\bar{c}}/\Gamma_{had}$ | $\Gamma_{b\bar{b}}/\Gamma_{had}$ |
|---|---|---|---|---|---|
| 2.0 | 0.1734 | 0.2226 | 0.2226 | 0.1710 | 0.2192 |
| 2.3 | 0.1733 | 0.2225 | 0.2225 | 0.1710 | 0.2188 |
| 3.0 | 0.1729 | 0.2219 | 0.2219 | 0.1710 | 0.2174 |
| 3.3 | 0.1733 | 0.2225 | 0.2225 | 0.1710 | 0.2188 |
| 4.0 | 0.1733 | 0.2224 | 0.2224 | 0.1710 | 0.2187 |

Table 2: *Quark fractions used to calculate the sample flavour purities.*

The errors on the purities fully take into account those from [7]. Monte Carlo studies indicate

| $-log_{10}(cut)$ | $\mathcal{P}_u$ | $\mathcal{P}_d$ | $\mathcal{P}_s$ | $\mathcal{P}_c$ | $\mathcal{P}_b$ |
|---|---|---|---|---|---|
| 2.0 | 2.8 $\pm$0.4 | 3.6 $\pm$0.5 | 3.6 $\pm$0.5 | 17.0 $\pm$0.8 | 73.0 $\pm$1.5 |
| 2.3 | 1.9 $\pm$0.3 | 2.4 $\pm$0.4 | 2.4 $\pm$0.4 | 14.4 $\pm$0.8 | 78.9 $\pm$1.4 |
| 3.0 | 0.9 $\pm$0.3 | 1.2 $\pm$0.4 | 1.2 $\pm$0.4 | 8.8 $\pm$0.7 | 88.0 $\pm$1.4 |
| 3.3 | 0.6 $\pm$0.2 | 0.8 $\pm$0.3 | 0.8 $\pm$0.3 | 6.9 $\pm$0.7 | 90.8 $\pm$1.3 |
| 4.0 | 0.3 $\pm$0.1 | 0.4 $\pm$0.2 | 0.4 $\pm$0.2 | 3.8 $\pm$0.6 | 95.2 $\pm$1.3 |

Table 3: *Purities of the quark flavours making up the samples of events used.*

that such a selection is highly efficient, yielding approximately 57% efficiency for tagging $b$-quarks in the angular acceptance defined by $cos\,\theta_{thrust} \leq 0.8$.

The current measurement makes no direct use of the the large ALEPH sample of simulated Monte Carlo events, however this has been used to indicate trends and estimate systematic errors. The sample consists of roughly 1.2 million simulated 1992 HVFLO3 events with additional smearing and weighting to take into account :

- The differing event vertex resolution from data and that used in generated events (1 versus 0.7 $cm$),
- The difference between the most recently measured $B$ lifetime and that used in the generation (1.3 versus 1.5 $ps$),
- The small additional impact-parameter smearing needed to correct the simulated resolution to that observed in data.

Unless otherwise specified, this sample is used throughout.

[4]The author is very grateful to Dave Brown (MPI Muenchen) for the use of these numbers.

# 4 Statistical Optimisation of $\kappa$ and Sample $b$-Purity

Currently the dominant uncertainty on $A_{FB}^{b\bar{b}}$ remains statistical and so the analysis may be optimised by minimising the statistical error. Systematic contributions are dealt with later and affect this statement only slightly. The optimisation is a two-dimensional one, in $\kappa$ and $b$-purity. The two parameters are almost completely independent[5] and so may be treated separately. The sensitivity of the total hadronic sample to an observable asymmetry may be written as :

$$\mathcal{S} = \sqrt{\frac{N(\mathcal{P}_b)}{\sigma_{FB}^2}} \sum_{f=u,d...}^{b} \delta_f C_f A_{FB}^f \mathcal{P}_f \tag{9}$$

where $N(\mathcal{P}_b)$ are the events selected[6] for a given $\mathcal{P}_b$. Relation (9) may be optimised as shown in Figure 1 to find the best working values for $\kappa$ and the $b$-purity. It is clear that a $\kappa$ of 0.5 at

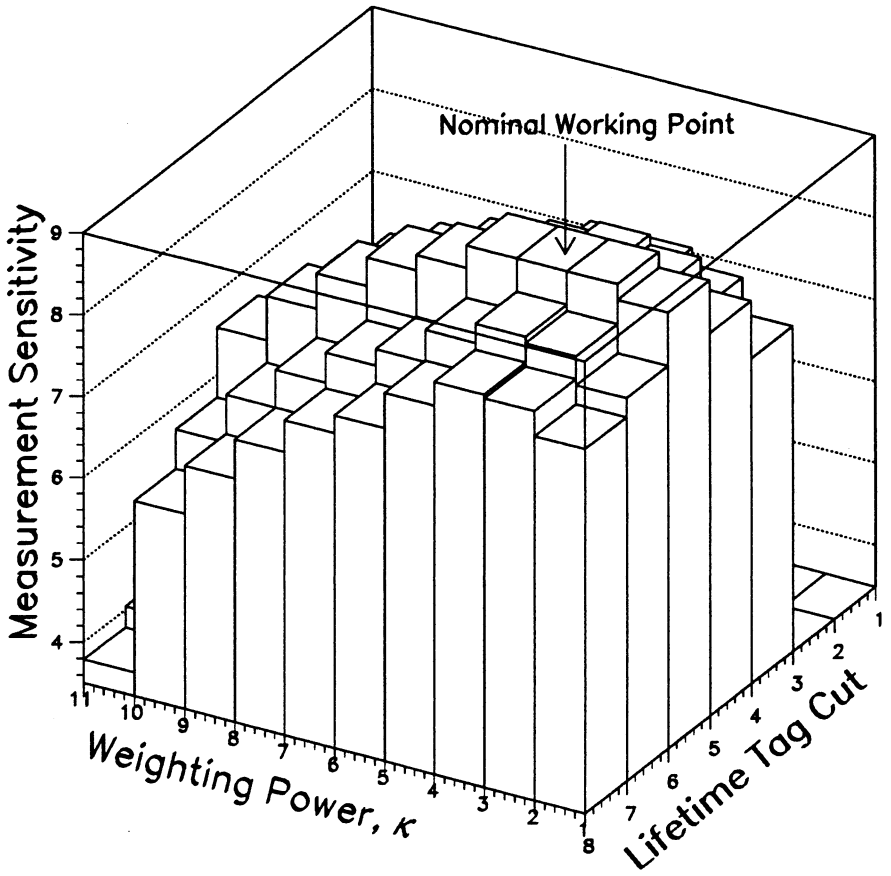


Figure 1: *Two-dimensional optimisation of the method's sensitivity as a function of $\kappa$ and the $b$-purity. The lifetime-tag cuts and $\kappa$ bins shown are those used throughout the analysis and given later in Table 4. Note the suppressed zero on the vertical scale.*

a $b$-purity of 88.0 ($\pm$1.4)% yields the most statistically significant asymmetry. The sensitivity is seen to have a fairly broad "plateau" in $\kappa$ and lifetime-tag cut around $\kappa$ values of 0.3 $\rightarrow$ 0.8 and 70 $\rightarrow$ 90% $b$-purity respectively. The previously [19] chosen values of :

$$\kappa = 0.5 \text{ and lifetime tag cut } = 10^{-3} \tag{10}$$

[5] There is a *small* correlation between the quark charge separations (the $\delta_f$'s) at fixed $\kappa$ and increasing $b$-purity. This is described in detail in [12]. The effect is negligible however for the current analysis.

[6] Currently assuming 1992 statistics for the moment.

are kept as the nominal working point at which $sin^2\theta_w^{eff}$ is extracted. This is done for reasons of consistency while it is clear that such a choice has little effect on the measured value. The fact that the optimal $\kappa$ value is not the same as that of the combined quark asymmetry and the jet-charge mixing analyses can be explained from studying the sensitivity of individual flavours [10].

# 5 Hemisphere Charge Asymmetry Measurements

Hemisphere-charge measurements are made using samples of events with an increasing $b$-purity as defined in Section 3. An additional requirement, that tracks used in the hemisphere-charge calculations have a $p_T > 200\,MeV/c$, is applied at this stage. This is done to remove badly reconstructed and looping tracks and to retain consistency with previous measurements [2, 11]. In addition, a full set of sagitta corrections for 1992 data are applied to those tracks used in the hemisphere-charge calculations [14].

The observed quantites in data are : $Q_{FB}$, $Q$ and $\bar{\delta}$ which are measured at the following values of $\kappa$ :

$$\kappa \;=\; 0.3,\, 0.4,\, 0.5,\, 0.7,\, 0.9,\, 1.0,\, 1.2, 1.5,\, 2.0,\, \infty \tag{11}$$

The intention of using such a range is to study systematic effects as a function of $\kappa$. This is a very powerful technique as $\kappa$ enters as a $p_L$-weighted *power*. The large range of $\kappa$ represents a complete scan over the charge and momentum spectra of hadronic jets which is in turn a severe test of the charge retention mechanism. A summary of the 1992 data measurements at different $\kappa$ and $b$-purities is given in Table 4. The asymmetry is clearly visible and is seen to increase in value as the $b$-purity of the sample becomes greater. These measurements are those used later to extract $A_{FB}^{b\bar{b}}$ and $sin^2\theta_w^{eff}$.

# 6 Acceptance for Lifetime-Tagged Events

An important parameter to interpret the asymmetry measurement is the ALEPH acceptance for lifetime-tagged events. This is apparent when considering :

$$A_{FB}\,(cos\,\theta_C) \;=\; \frac{\sigma^f \,-\, \sigma^{\bar{f}}}{\sigma^f \,+\, \sigma^{\bar{f}}} \tag{12}$$

where $\theta_C$ represents the maximum value of $cos\,\theta_{thrust}$ allowed. The efficiency corrected contributions are :

$$\sigma^f \;=\; \int_0^{cos\,\theta_C} \left[\tfrac{3}{8}\,(1 \,+\, cos^2\theta) \,+\, A_{FB}^{f\bar{f}}\,cos\,\theta\right] \sigma_{had}\,\frac{\Gamma_f}{\Gamma_{had}}\,\epsilon_f^e\,(cos\,\theta)\;\partial\,cos\,\theta \tag{13}$$

$$\sigma^{\bar{f}} \;=\; \int_0^{cos\,\theta_C} \left[\tfrac{3}{8}\,(1 \,+\, cos^2\theta) \,-\, A_{FB}^{f\bar{f}}\,cos\,\theta\right] \sigma_{had}\,\frac{\Gamma_{\bar{f}}}{\Gamma_{had}}\,\epsilon_{\bar{f}}^e\,(cos\,\theta)\;\partial\,cos\,\theta \tag{14}$$

where $\epsilon_{f\bar{f}}^e\,(cos\,\theta_C)$ is the event selection efficiency[7]. Ignoring all angular-independent terms and assuming the purity to be uniform in $cos\,\theta_{thrust}$, yields :

$$A_{FB}\,(cos\,\theta_C) \;=\; \frac{\int_0^{cos\,\theta_C} 2\,A_{FB}\,cos\,\theta\,\epsilon_{f\bar{f}}^e\,(cos\,\theta)\;\partial\,cos\,\theta}{\int_0^{cos\,\theta_C} \frac{3}{4}\,(1 \,+\, cos^2\theta)\,\epsilon_{f\bar{f}}^e\,(cos\,\theta)\;\partial\,cos\,\theta} \tag{15}$$

where it is clear that the absolute normalisation of $\epsilon_{f\bar{f}}^e\,(cos\,\theta)$ is unimportant and it is only the *shape* which is relevant. This depends upon the angle of quark jets within ALEPH. The acceptance is essentially determined by the cylindrical geometry of VDET, convoluted with the jet opening-angle distribution. VDET consists of two concentric cylinders extending to $\pm 0.69$ and $\pm 0.84$ in $cos\,\theta$ respectively. The normalised efficiency is shown as a function of $cos\,\theta_{thrust}$ in Figure 2. Data and Monte Carlo distributions agree over the full range of lifetime-tag cuts

[7] Assumed to be equal for both the fermion going forward ($f$) and backward ($\bar{f}$).

| *Sample b-Purity of 21 %* | | | | | | |
|---|---|---|---|---|---|---|
| $\kappa$ | $Q_{FB}$ *and Error* | | $Q$ *and Error* | | $\delta$ *and Error* | |
| 0.30 | -0.00396 | 0.00047 | 0.00754 | 0.00037 | 0.2033 | 0.0009 |
| 0.40 | -0.00460 | 0.00051 | 0.00728 | 0.00041 | 0.2110 | 0.0010 |
| 0.50 | -0.00524 | 0.00055 | 0.00706 | 0.00046 | 0.2217 | 0.0012 |
| 0.70 | -0.00650 | 0.00066 | 0.00669 | 0.00057 | 0.2478 | 0.0016 |
| 0.90 | -0.00768 | 0.00078 | 0.00641 | 0.00068 | 0.2750 | 0.0020 |
| 1.00 | -0.00822 | 0.00084 | 0.00630 | 0.00073 | 0.2878 | 0.0022 |
| 1.20 | -0.00921 | 0.00095 | 0.00613 | 0.00084 | 0.3109 | 0.0026 |
| 1.50 | -0.01043 | 0.00109 | 0.00594 | 0.00098 | 0.3389 | 0.0032 |
| 2.00 | -0.01187 | 0.00127 | 0.00573 | 0.00116 | 0.3707 | 0.0040 |
| $\infty$ | -0.01385 | 0.00204 | 0.00527 | 0.00194 | 0.4378 | 0.0091 |
| *Sample b-Purity of 88 %* | | | | | | |
| $\kappa$ | $Q_{FB}$ *and Error* | | $Q$ *and Error* | | $\delta$ *and Error* | |
| 0.30 | -0.00883 | 0.00101 | 0.00515 | 0.00083 | 0.1558 | 0.0021 |
| 0.40 | -0.01004 | 0.00110 | 0.00487 | 0.00093 | 0.1600 | 0.0025 |
| 0.50 | -0.01123 | 0.00122 | 0.00460 | 0.00105 | 0.1670 | 0.0030 |
| 0.70 | -0.01345 | 0.00150 | 0.00408 | 0.00133 | 0.1859 | 0.0041 |
| 0.90 | -0.01544 | 0.00180 | 0.00359 | 0.00163 | 0.2070 | 0.0054 |
| 1.00 | -0.01634 | 0.00195 | 0.00333 | 0.00177 | 0.2173 | 0.0060 |
| 1.20 | -0.01792 | 0.00223 | 0.00282 | 0.00205 | 0.2363 | 0.0074 |
| 1.50 | -0.01979 | 0.00261 | 0.00205 | 0.00243 | 0.2598 | 0.0092 |
| 2.00 | -0.02184 | 0.00312 | 0.00086 | 0.00293 | 0.2865 | 0.0121 |
| $\infty$ | -0.02339 | 0.00537 | -0.00152 | 0.00524 | 0.3135 | 0.0339 |
| *Sample b-Purity of 95 %* | | | | | | |
| $\kappa$ | $Q_{FB}$ *and Error* | | $Q$ *and Error* | | $\delta$ *and Error* | |
| 0.30 | -0.00978 | 0.00121 | 0.00433 | 0.00099 | 0.1490 | 0.0025 |
| 0.40 | -0.01111 | 0.00132 | 0.00400 | 0.00111 | 0.1534 | 0.0030 |
| 0.50 | -0.01238 | 0.00147 | 0.00366 | 0.00126 | 0.1607 | 0.0036 |
| 0.70 | -0.01473 | 0.00181 | 0.00294 | 0.00161 | 0.1802 | 0.0050 |
| 0.90 | -0.01671 | 0.00218 | 0.00220 | 0.00197 | 0.2018 | 0.0066 |
| 1.00 | -0.01757 | 0.00237 | 0.00181 | 0.00215 | 0.2122 | 0.0074 |
| 1.20 | -0.01904 | 0.00272 | 0.00104 | 0.00249 | 0.2316 | 0.0090 |
| 1.50 | -0.02068 | 0.00319 | -0.00008 | 0.00296 | 0.2555 | 0.0113 |
| 2.00 | -0.02235 | 0.00381 | -0.00174 | 0.00358 | 0.2827 | 0.0148 |
| $\infty$ | -0.02376 | 0.00664 | -0.00448 | 0.00648 | 0.3052 | 0.0430 |

Table 4: *Values of the Measurable quantities in data as a function of $\kappa$ and b-purity for the 1992 data.*

given in Table 3. The statistical and systematic differences between data and Monte Carlo are used later to estimate the systematic contribution to $A_{FB}^{b\bar{b}}$ coming from the precise knowledge of these shapes.

The $A_{FB}^{b\bar{b}}$ measurement always contains some fraction of "background" events from other quark flavours. To accurately correct for these contributions, it is important to understand how the shape of the angular acceptance depends on flavour. The efficiencies are shown in Figure 3 for different quark types. As is shown in Figure 3 (a), the shape of the total tagging efficiency in data is dominated by the $b$ tagging efficiency and is in close agreement with that expected from Monte Carlo. The total acceptance is dominated by $\epsilon_{b\bar{b}}^{e}$ as $\mathcal{P}_b \gg \mathcal{P}_{u,d,s,c}$ and so the *measured* total efficiency as a function of $\cos\theta_{thrust}$ strongly constrains the dominant flavour-dependent

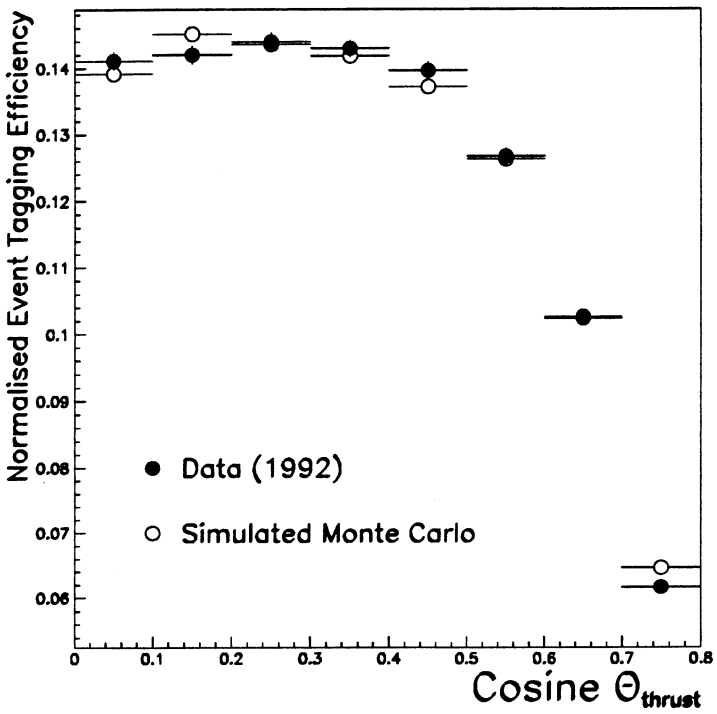


Figure 2: *Normalised efficiency to select lifetime-tagging events as a function of the thrust angle for data and simulated events. Note the supressed zero.*

acceptance factor, $C_b$. The statistical and systematic errors on $A_{FB}^{b\bar{b}}$ arising from the acceptance factors, remain small as a result. They are discussed in more detail in Section 9.2. The slightly different behaviour of each quark may be understood as arising from :

*b* events possess a relatively large amount of "lifetime" distributed fairly widely throughout more spherical jets. Hence, when approaching the edge of the VDET acceptance, some tracks may be lost whilst still allowing the event to tag.

*c* events possess a smaller amount of lifetime. This is centered along the axis of narrower jets so that, close to the edge of VDET acceptance, they rapidly lose the ability to tag and their efficiency drops more quickly at low angles.

$u, d, s$ events possess lifetime largely through the presence of long lived particles such as $K^0$'s and $\Lambda$'s which are spread *throughout* the jets. As each event has a small amount of lifetime information, which is only loosely correlated with the jet direction, these events lose tagging efficiency monotonically from the centre of the detector.

For the same reasons, the shape of the curves also depends on the lifetime-tag cut applied, as the relative importance of each of the above depends on the number of tracks and amount of lifetime which is required to tag.

# 7 Parameterisation of the Acceptance and Selection of $cos\,\theta_C$

The flavour-dependent acceptances are characterised by a "flat" region in the centre of VDET where the jet-core is well-contained and a region where the efficiency starts to fall as the lifetime information in the jet is lost down the beam-pipe. The choice of an optimal $cos\,\theta_C$ is made by considering the variation of the various $C_f$'s as a function of $cos\,\theta_C$. The $C_f$'s are calculated

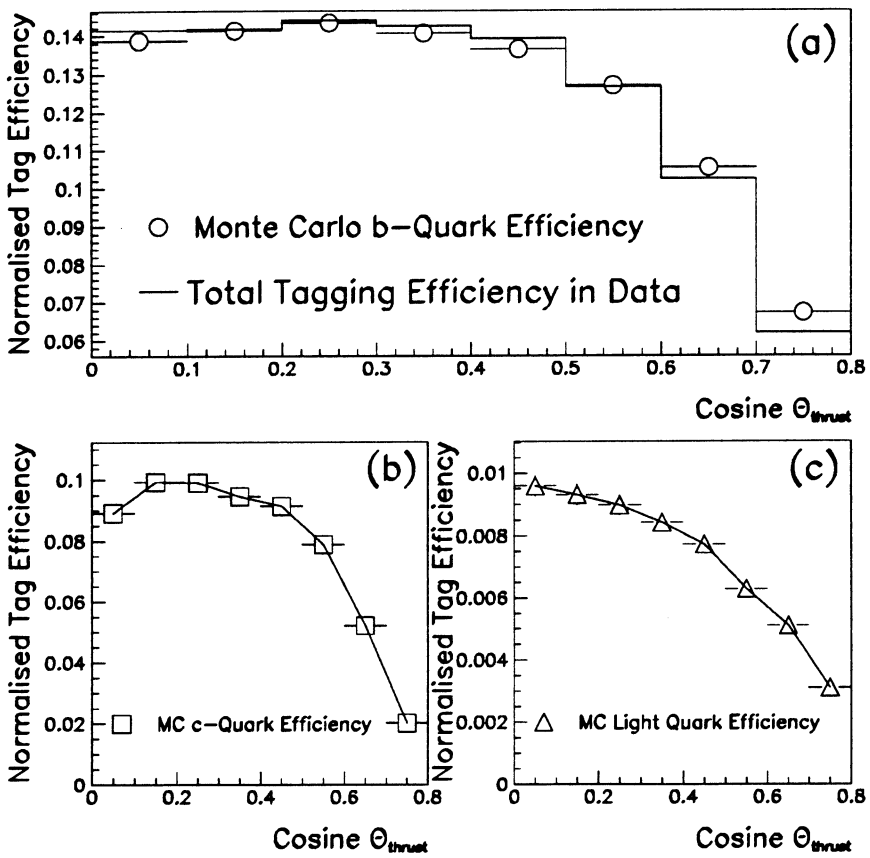


Figure 3: *Normalised efficiency to select lifetime-tagging events as a function of angle for (a) b quark events, (b) c quark events and (c) for light quark flavours* $(u, d, s)$. *Note the suppressed zero in (a) where the b tagging efficiency in Monte Carlo is compared with the* total *tagging efficiency in data.*

from a linear extrapolation between bins of efficiency plots of tje type shown in Figure 3. These are then used to integrate over the full range of $cos\,\theta$ up to the maximum $cos\,\theta_C$. Assuming $cos\,\theta \equiv x$ for ease of notation then this gives a bin-by-bin acceptance contribution of :

$$C_f = \frac{\sum_{bins}^{x_1 \to x_2} \left[ P_1 x^2 + \frac{2}{3} P_2 x^3 \right]_{x_1}^{x_2}}{\sum_{bins}^{x_1 \to x_2} \left[ \frac{3}{4} P_1 x + \frac{3}{8} P_2 x^2 + \frac{P_1}{4} x^3 + \frac{3}{16} P_2 x^4 \right]_{x_1}^{x_2}} \tag{16}$$

where :

$$P_1 = \epsilon_1 - P_2 x_1 \quad \text{and} \; P_2 = \frac{\epsilon_1 - \epsilon_2}{x_1 - x_2} \tag{17}$$

with $(\epsilon_1, \epsilon_2)$ and $(x_1, x_2)$ the efficiency and $cos\,\theta$ boundaries respectively. This is shown in Figure 4 for the nominal $b$-purity which indicates that the limited VDET acceptance does not increase the observable asymmetry $(C_b)$ beyond a $cos\,\theta$ of 0.8. The curves remain roughly parallel all flavours and lifetime-tag cuts. There is a 3% drop in the acceptance at the highest $b$-purity for the $b$ quarks due to the dependence on the multiplicity of tracks passing through VDET. Figure 4 shows that there is a 3.2% increase in $C_b$ by moving from a $cos\,\theta_C$ of $0.7 \rightarrow 0.8$ with only a 0.4% increase in moving from $0.8 \rightarrow 0.9$. This indicates that nothing more to be gained by going beyond a $cos\,\theta_C$ of 0.8 usimg the current version of VDET and QIPBTAG[8].

[8]This is likely to change with the new version of the tagging algorithm.

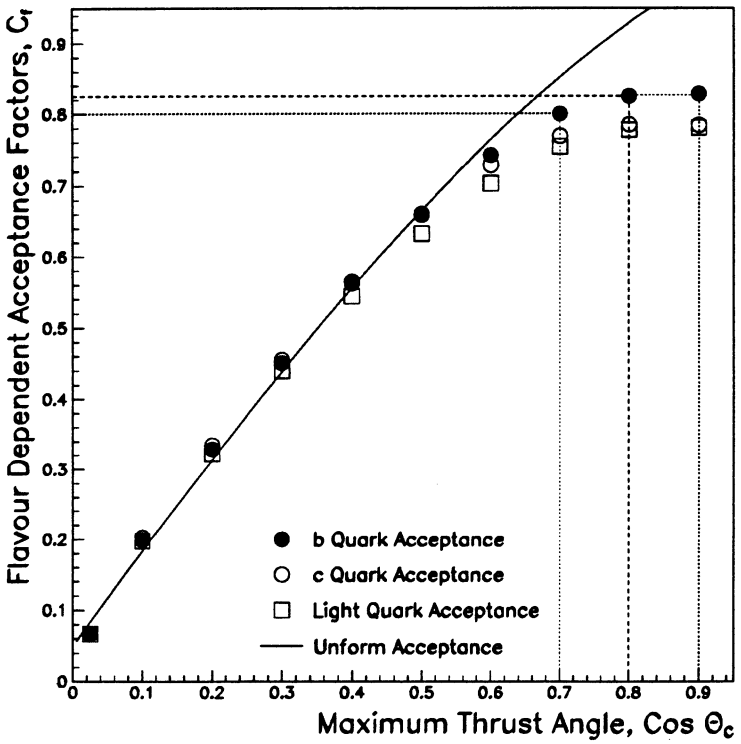


Figure 4: *Variation of the $C_f$ of b, c and light flavours as a function of the maximum $\cos\theta$ cut. The solid line represents the case where the acceptance is flat in $\cos\theta$ and is shown for comparison.*

Choosing an optimal cos $\theta_C$ is complicated by the fact that the purity calculations of Section 3 are derived for the region $|\cos\theta_{jet}| \leq 0.7$. Any extrapolation beyond this $\cos\theta$ must be chosen with care. By construction, the lifetime-tag tends to yield a uniform $b$-purity distribution in $\cos\theta$ when events are fully contained by the VDET. Consequently, the purity is assumed to be a constant within the angular acceptance used by the asymmetry measurement. However, this response is slightly distorted by the behaviour of quarks close to the edge of the VDET acceptance. The efficiency distributions of Figure 3 indicate that the tagging for $b$ quarks is more persistent at large angles than those of lighter flavours when jets are only partially inside VDET. The change in the average flavour purities in Monte Carlo events are shown in Figure 5 and indicate that this effect manifests itself as a slight increase in the $b$-purity in the region of $\cos\theta$ between $0.7 \rightarrow 0.8$. The effect of this small increase on $\langle Q_{FB}^{btag} \rangle$ may be conservatively[9] estimated using :

$$\frac{\Delta\langle Q_{FB}^{btag}\rangle}{\langle Q_{FB}^{btag}\rangle} = \left[C_b \frac{\Delta\mathcal{P}_b}{\mathcal{P}_b}\right]_{\cos\theta=0.7}^{\cos\theta=0.8} \tag{18}$$

where, for example, $\Delta\mathcal{P}_b/\mathcal{P}_b$ is the relative change in $b$-purity estimated from the Monte Carlo. In the case of the curves shown in Figure 5 and taking into account the acceptance curves in Figure 4 indicates that such effects remain at the level of $\Delta\langle Q_{FB}^{btag}\rangle \sim 10^{-5}$ or well below the 1% level of $\langle Q_{FB}^{btag}\rangle$. This is taken into account in the fitting procedure described later in Section 9. It is treated in a similar way to relation (18) in that the bin-by-bin integrated acceptance factors are modified to take into account the angular deviations of the purity from the value measured in data up to $\cos\theta$ of 0.7. As a systematic cross-check, the curves of Figure 5 are used in the

[9]This is conservative because the purities of the lighter quark flavours are also *reduced* whilst their effect is mostly to cancel the measured $A_{FB}^{bb}$.

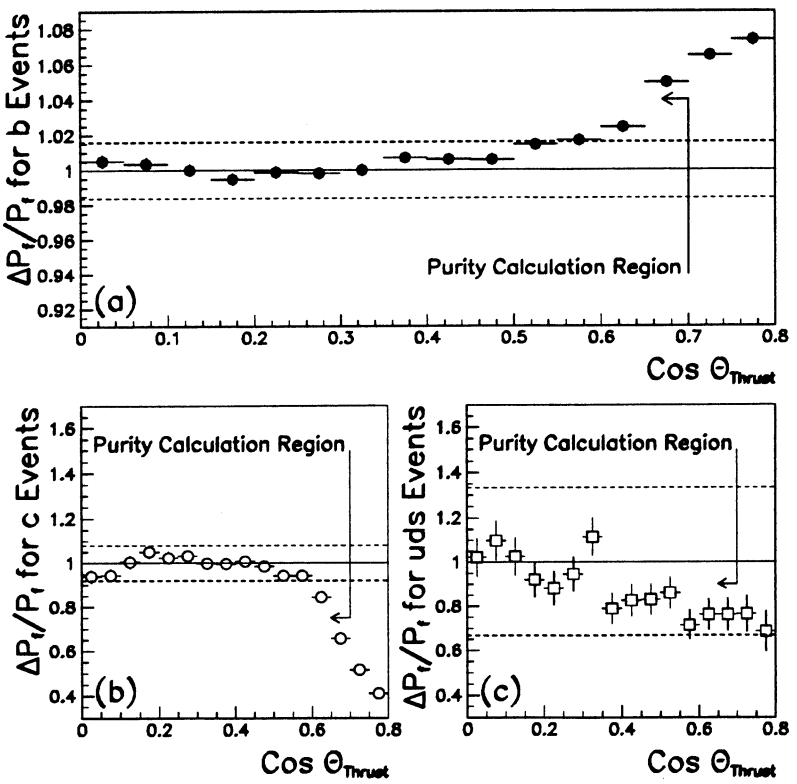


Figure 5: *Relative change in the quark purities as a function of angle in simulated events. Figure (a) shows the behaviour for b quarks while Figures (b) and (c) shows those for c and light quark flavours respectively. The horizontal bands indicate the statistical and systematic uncertainty assumed for the purities which are used later in the fit and error determination. These curves are for the case when* $\mathcal{P}_b$ *is* $88.0(\pm 1.4)\%$.

fits and 10% of their total effect taken as the systematic error.

To conclude; in order to minimise the systematic error in the extrapolation of sample purities from the $|\cos\theta_{jet}| \leq 0.7$ acceptance, and to maximise the measurable asymmetry, $\cos\theta_C$ is fixed at :

$$\cos\theta_C = 0.8 \tag{19}$$

for the purposes of the current measurement and lifetime-tag.

# 8 Calibration of the Hemisphere Charge Method for $b$ Quarks

There are currently two measurements of $\delta_b$ available from data. If used, they suppress fragmentation uncertainties from the other quarks by more[10] than the factor $\mathcal{P}_b$. Measurements are made using the lepton-signed hemisphere-charge method and using the difference between the $Q_{FB}^{btag}$ and $Q^{btag}$ distribution widths to extract $\bar{\delta}_b$ and hence $\delta_b$. The latter will be referred to here as $\delta_b^{widths}$ whilst the lepton-signed hemisphere-charge method is denoted by $\delta_b^{lepton}$. The two methods are described in detail in [11, 12] and their results are summarised in Table 5. The lepton results are *preliminary* however, and will be updated in the near future. As a result, the combined values are given in Figure 6 for reference purposes but only the $\delta_b^{widths}$ measurements are used for the fit results given later. Both methods yield *independent* measurements of $\delta_b$ accurate to roughly $3 \rightarrow 5\%$ which are combined to reach an average $\delta_b^{combined}$ with an

[10] After cancellations between the various flavours are taken into account.

| $\kappa$ | $\delta_b^{widths}$ from Lifetime-Tag | | | | $\delta_b^{lepton}$ from Lepton-Tag | | | | |
|---|---|---|---|---|---|---|---|---|---|
| | $\delta_b^{widths}$ | $\pm$ *stat.* | $\pm$ *syst.* | $\pm$ *Total* | $\delta_b^{leptons}$ | $\pm$ *stat.* | $\pm$ *syst.* | $\pm \Delta\chi$ | $\pm$ *Total* |
| 0.3 | 0.1104 | 0.0026 | 0.0040 | 0.0048 | | | | | |
| 0.4 | 0.1254 | 0.0027 | 0.0041 | 0.0049 | | | | | |
| 0.5 | 0.1405 | 0.0024 | 0.0033 | 0.0049 | 0.1466 | 0.0042 | 0.0038 | 0.0042 | 0.0071 |
| 0.7 | 0.1695 | 0.0030 | 0.0039 | 0.0060 | 0.1737 | 0.0052 | 0.0043 | 0.0050 | 0.0084 |
| 0.9 | 0.1956 | 0.0045 | 0.0063 | 0.0077 | | | | | |
| 1.0 | 0.2079 | 0.0040 | 0.0052 | 0.0083 | 0.2099 | 0.0068 | 0.0054 | 0.0060 | 0.0106 |
| 1.2 | 0.2280 | 0.0058 | 0.0079 | 0.0095 | | | | | |
| 1.5 | 0.2523 | 0.0059 | 0.0063 | 0.0113 | 0.2532 | 0.0092 | 0.0069 | 0.0072 | 0.0136 |
| 2.0 | 0.2779 | 0.0088 | 0.0154 | 0.0178 | | | | | |
| $\infty$ | 0.2873 | 0.0148 | 0.0119 | 0.0331 | 0.3345 | 0.0189 | 0.0100 | 0.0096 | 0.0234 |

Table 5: *Summary of the* ALEPH $\delta_b$ *measurements in data.*

| $\kappa$ | $\delta_b^{combined}$ *and Errors* | | | | | *Weights* | |
|---|---|---|---|---|---|---|---|
| | $\delta_b^{combined}$ | $\pm$ *Total* | $\pm$ *stat.* | $\pm$ *syst.* | $\pm$ *stat.* $\oplus \pm$ *syst.* | $W(\delta_b^{leptons})$ | $W(\delta_b^{widths})$ |
| 0.5 | 0.1425 | 0.0040 | 0.0024 | 0.0033 | 0.0040 | 20112.63 | 40966.82 |
| 0.7 | 0.1709 | 0.0049 | 0.0030 | 0.0039 | 0.0049 | 14178.36 | 27048.96 |
| 1.0 | 0.2087 | 0.0065 | 0.0040 | 0.0052 | 0.0065 | 8976.66 | 14513.79 |
| 1.5 | 0.2527 | 0.0087 | 0.0059 | 0.0063 | 0.0087 | 5432.13 | 7903.26 |
| $\infty$ | 0.3187 | 0.0191 | 0.0148 | 0.0119 | 0.0190 | 1820.27 | 912.73 |

Table 6: *Summary of the combined values of* $\delta_b$ *from the values given in the previous Table. The total, statistical and systematic errors are given together with the relative weights of the two types of measurement.*

overall precision of better than 2.6%. The lepton-signed hemisphere-charge method contains a systematic error due to the uncertainty from the mixing of the lepton used to give the "reference charge" to the hemisphere opposite it. In the current notation, this error is absorbed into the total systematic error when making the average $\delta_b^{combined}$. It is important to note that this is the only point at which $\chi$ enters the analysis. Both the asymmetry and $\delta_b^{widths}$ measurements *automatically* contain the "correct" mixing fraction and the degree of charge dilution this creates in $b$ quark jets. The uncertainty on $\delta_b^{combined}$ from $\chi$ is then suppressed by the weight with which $\delta_b^{lepton}$ contributes relative to that of $\delta_b^{widths}$. This leads to an small, but opposite, dependence[11] of the extracted $A_{FB}^{b\bar{b}}$ on $\chi$ as is found in lepton asymmetry measurements [15]. This is discussed later in Section 9.2 whilst the current weights are shown in Table 6.

An additional consideration must be taken into account when using the hemisphere-charge technique with the lifetime-tag, QIPBTAG. This concerns the small lifetime dependence of the quark $\delta_f$'s. The lifetime-tag affects hemisphere-charge calculations by selecting events with a slightly increased charged multiplicity and average track momentum. These kinematical effects alter the widths and means of hemisphere-charge distributions [12]. However in the asymmetry formalism used here, it is only the mean $\delta_f$'s which are relevant. The distribution widths only enter when considering the statistical significance of the $A_{FB}^{b\bar{b}}$ measurement which is observed in the data. The corrections which must be applied to the mean $\delta_f$'s are shown in Figure 6 as a function of the $b$-purity at which the measurement is performed. The effects are generally small and become more so for heavy flavoured quarks. The corrections are typically $\sim$ 2% for the

[11] This is currently over 2.5 times smaller than that of competitive high-$p_T$ lepton measurements.

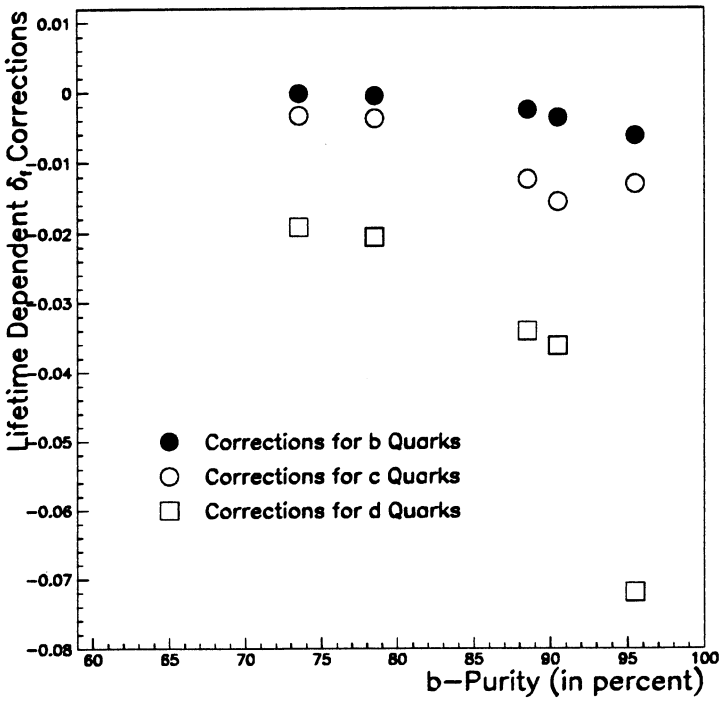


Figure 6: *Lifetime dependent corrections which are applied to the various quark separations as a result of kinematical selection of the lifetime-tag for different b-purity . The values shown are for a $\kappa$ of 0.5.*

dominant, $\delta_b$, contribution. The statistical error on the lifetime dependent corrections are used as a systematic error. These lead to a negligible uncertainty on the $\delta_f$'s.

# 9 Extraction of $A_{FB}^{b\bar{b}}$ and $sin^2\theta_w^{eff}$

The extraction of $A_{FB}^{b\bar{b}}$ and $sin^2\theta_w^{eff}$ from the measured asymmetries of Section 5 is performed essentially using equation (4). The input quantities, $\delta_f$, $\mathcal{P}_f$, $C_f$, are combined with theoretical expectations of $A_{FB}^{f\bar{f}}$ and compared with the measured $\langle Q_{FB}^{btag}(\kappa, \mathcal{P}_b)\rangle$. At high $b$-purity the measurement is essentially that of $A_{FB}^{b\bar{b}}$ with small "background" corrections for other quark flavours. The statistical and systematic errors on $A_{FB}^{b\bar{b}}$ and $sin^2\theta_w^{eff}$ are calculated within this context and ensure that the errors on the $\delta_f$'s, $\mathcal{P}_f$'s and $C_f$'s are treated in the same way as the measurement itself. This places some demands and constraints on the way the fitter is implemented which are explained in Section 9.1. The details of the systematic error calculations are given in Section 9.2.

## 9.1 The Fitter Implementation

The ZFITTER [16] package is used to calculate the $A_{FB}^{f\bar{f}}$'s within the context of the Standard Model. In the lowest-order SM , all quark asymmetries are determined by a single parameter, $sin^2\theta_w$. However, higher-order radiative electroweak corrections depend on all parameters of the SM, in particular on the unknown parameters $m_t$ and $M_H$. Within the on-shell renormalisation scheme, the corrections have a structure that allow their absorbtion into a redefinition of $sin^2\theta_w$. It is this *effective* weak mixing angle, $sin^2\theta_w^{eff}$, that determines the asymmetries at the Z peak.

The convention adopted here and elsewhere [1, 16] is that :

$$sin^2\theta_w^{eff} = \left(sin^2\theta_w^{eff}\right)^{leptons} \tag{20}$$

as the radiative corrections to each fermion process are flavour dependent. The correspondence between $sin^2\theta_w^{eff}$ and $A_{FB}^{b\bar{b}}$ is one-to-one and so may be considered to be synonymous within the fitting procedure. $m_t$ is used as a convenient way to vary $sin^2\theta_w^{eff}$ within ZFITTER. The Higgs mass used for these calculations is maintained at $M_H = 300$ GeV throughout.

Although dominated by the $b$-channel, equation (4) contains multiple dependencies on $sin^2\theta_w^{eff}$ from the various quark flavours. Consequently it is most easily solved iteratively. This is equivalent to "assuming a Standard Model relation" between $A_{FB}^{b\bar{b}}$ and $A_{FB}^{c\bar{c}}$ and the lighter or "background" quark asymmetries [1]. This means that the leading particle effects of the backgound asymmetry are taken into account correctly as it also contains a small $sin^2\theta_w^{eff}$ dependence. The asymmetries of the different quark flavours all have slightly different vertex corrections but in practice the differences are very small, and are negligible for the current precision of measurement.

A fully iterative solution of equation (4) to a precision greater than that required by some of the smaller systematic error contributions ($\Delta sin^2\theta_w^{eff} \approx 10^{-4}$) requires a large number of complex calculations. Version 4.5 of ZFITTER is used to calculate the $A_{FB}^{f\bar{f}}$'s using the SM "branch" of the calculations. In order to reduce the time required to calculate a single, expected $\langle Q_{FB}^{btag}\rangle$ value, the calculations are performed over a large grid of $sin^2\theta_w^{eff}$ and $A_{FB}^{b\bar{b}}$ values and are stored for the different energies used in the corresponding LEP run period. A weighting scheme is then used to correct for the spread of energies and data samples used in the fit. This is sufficiently accurate due to the approximately linear behaviour of $A_{FB}^{b\bar{b}}$ as a function of energy in the regime close to the Z peak. A further linear interpolation is then used to restrict a small range of $\pm\frac{1}{3}\sigma$ surrounding the expected value which is then scanned[12]. This method is found to yield the required precision with a speed which makes it acceptable also for calculating the systematic errors in an efficient manner.

## 9.2 Systematic Error Contributions

The manner in which the systematic errors on $A_{FB}^{b\bar{b}}$ and $sin^2\theta_w^{eff}$ are treated depends somewhat on their source. All systematic errors have been calculated for all the values of $\kappa$ and lifetime-tag cut used in the analysis. They are discussed here separately in approximate order of importance :

(i) *Errors arising from uncertainties on $\delta_b$ :* These may be separated into the categories of : (a) the statistical error on $\delta_b^{combined}$, (b) the systematic error on $\delta_b^{combined}$ and (c) the $\chi$ dependent uncertainty of the $\delta_b^{lepton}$ contained in $\delta_b^{combined}$ measurement, (d) the lifetime dependent corrections on $\delta_f$'s. All these errors are passed through to $A_{FB}^{b\bar{b}}$ and $sin^2\theta_w^{eff}$ by smearing their input values to the electroweak fit using normal distributions with the appropriate $1\sigma$ widths. The $\chi$ uncertainty is separated from the other systematic error sources due to the opposite dependence it creates for the current measurement of $A_{FB}^{b\bar{b}}$ and that from leptons [15].

(ii) *Experimental systematics on $\langle Q_{FB}^{btag}\rangle$ :* These arise from several sources and are included simply in the manner of an "additional statistical" error on $\langle Q_{FB}^{btag}\rangle$ . The errors are calculated in a procedure similar to that of the combined hadronic asymmetry [17]. This involves a study of the sensitivity of $\langle Q_{FB}^{btag}\rangle$ to charged tracks at the edge of the track selection cuts applied for the hemisphere-charge calculations [18]. In addition, the sagitta corrections which are applied as a function of $cos\,\theta$ are maximally distorted[13] and the

[12] A comparison of the results from this method with that obtained using a full scan of complete calculations yield identical results.

[13] The corrections for the positively charged tracks are systematically shifted by $+1\sigma$ while those of negatively charged tracks are reduced by $-1\sigma$.

effect on $\langle Q_{FB}^{btag} \rangle$ taken as a systematic uncertainty from the corrections. The effects of using or removing anomalously high-momentum tracks are also used. Finally, the effects of any potential material asymmetry are inferred from the asymmetry in photon conversions combined with the mean *total* charge, $\langle Q^{btag} \rangle$. The error on any of the observed shifts are taken in conjunction with the magnitude of the shift itself to obtain the total systematic uncertainty. Similarly, any correlations between track selection cuts[14] are ignored yielding a highly conservative estimate.

(iii) *Errors arising from uncertainties in flavour-purities :* These are dominated by the uncertainties on $\mathcal{P}_b$ which are derived from those of the lifetime-tagged $\Gamma_{b\bar{b}}$ analysis. These have been studied in detail in [7] and are propagated to $\mathcal{P}_b$ via the relation that any uncertainty on the measured $\Gamma_{b\bar{b}}$ is proportional to that on the $b$-tagging efficiency and hence of the $b$-purity via relation (8). The statistical and systematic errors are added in quadrature and are smeared by normal distributions of the corresponding width in the electroweak fitting procedue.

(iv) *Theoretical uncertainties on* QCD *corrections to* $A_{FB}^{b\bar{b}}$ *:* These arise from an incomplete knowledge of how gluon radiation affects the angular distribution of the primary $f\bar{f}$ directions when reconstructed using a thrust-axis algorithm. The *explicit* QCD corrections are of the form :

$$\left(A_{FB}^{b\bar{b}}\right)_{measured} = \left(A_{FB}^{b\bar{b}}\right)_{uncorrected} \left[1 - k\frac{\alpha_s}{\pi}\right] \tag{21}$$

where $k$ is an experimentally determined quantity which depends on flavour and the type of algorithm which is used to reconstruct the primary $f\bar{f}$ directions within the detector. The current measurement is made using the thrust axis which essentially operates as a "semi-infinite $y_{cut}$" jet-finding algorithm. This implies that the sensitivity to such QCD corrections is likely to be very small. This has been studied [20] with the preliminary conclusion that it is only effects of the finite thrust axis *resolution*, for events lying close to the $cos\,\theta = 0$ boundary, which are of importance. These studies are to be documented in a forthcoming ALEPH note and indicate a correction due to the thrust axis resolution of 0.7% of $A_{FB}^{b\bar{b}}$ and a total uncertainty, *even if* a full explicit QCD correction had to be applied, of 1%. The approach employed here is to perform the fit *without* applying explicit QCD corrections within ZFITTER[15] and to assign a systematic uncertainty of :

$$\left(\frac{0.7\%}{2} \times A_{FB}^{b\bar{b}}\right) = \left(\Delta sin^2\theta_w^{eff}\right)_{no\,\mathrm{QCD}} = \pm 0.00008 \tag{22}$$

as a $\kappa$ and $\mathcal{P}_b$ dependent error on $A_{FB}^{b\bar{b}}$ and $sin^2\theta_w^{eff}$. So no correction is applied, but a systematic uncertainty is assigned with $\frac{1}{2}$ the value of the total effect of the thrust axis resolution.

(v) *Fragmentation statistical and systematic uncertainties :* These are due to leading particle effects in the "background" asymmetry from the lighter quark flavours. The $(u, d, s, c)$ mean hemisphere-charges ($\delta_f$'s) are taken from Monte Carlo with a systematic error calculated from their dependence on varying the various JETSET model parameters given in Table 7. The systematic error is conservatively estimated by summing in quadrature the effects on each of the background flavour asymmetries after each parameter variation. The sizeable correlations between parameter variations and flavours are ignored in order to arrive at a conservative estimate. The statistics from the Monte Carlo together with the lifetime dependence of the background $\delta_f$'s are also included in the total error.

[14] For example, those that certainly exist between $(D_0, Z_0)$ and $(p_T, cos\,\theta, N_{TPC\,hits})$.

[15] This is equivalent to performing the calculations with $\alpha_s = 0$ which assumes that a full-correction has to be applied. ie. ignoring the gluon fragmentation products in the detctor axis reconstruction.

| *Model Parameter* | *Parameter Range* | |
|---|---|---|
| $\lambda_{QCD}$ | 0.296 | 0.346 |
| $M_{min}$ | 1.530 | 1.770 |
| $\sigma$ | 0.342 | 0.352 |
| $\epsilon_b$ | 0.002 | 0.007 |
| $V/(V+PS)_{u,d}$ | 0.520 | 0.580 |
| $V/(V+PS)_s$ | 0.570 | 0.630 |
| $V/(V+PS)_{c,b}$ | 0.510 | 0.690 |
| $\frac{s}{u}$ | 0.291 | 0.311 |
| $\chi_d$ | 0.118 | 0.180 |
| $\chi_s$ | 0.250 | 0.499 |
| *Baryon Fraction* | 0.099 | 0.110 |
| *Popcorn Parameter* | 0.350 | 0.550 |

Table 7: *The list of* JETSET *fragmentation parameters varied in order to calculate the systematic error on the charge retention in the "background" asymmetry contributions to the dominant* $A_{FB}^{b\bar{b}}$ *asymmetry.*

(vi) *Angular Efficiency Systematic and Statistical Uncertainties:* These are calculated firstly from the statistical uncertainty in the angular flavour tagging efficiencies shown, for example in Figure 3, from the Monte Carlo. The systematic error on the flavour acceptances are then calculated from the scaled difference between the data and Monte Carlo *total tagging efficiency*, using the purities of Table 3. These are then varied on a bin-by-bin basis and the acceptance factors recalculated. Their total effect on the extracted $sin^2\theta_w^{eff}$ and $A_{FB}^{b\bar{b}}$ are then taken as the RMS of the resulting distributions. An additional consideration, which is discussed in Section 7, is that of the purity variation in the $cos\,\theta$ region between 0.7 and 0.8. This region is not included in the calibration of the tag purities. Using a suitable reweighting of the acceptance factors, to take the Monte Carlo prediction for this region into account, an estimate of the effect of including this region is made. The systematic uncertainty on this prediction is taken as ±10% of this effect.

# 10 Summary of Results and Errors

The statistical and systematic errors on $A_{FB}^{b\bar{b}}$ are shown in Figure 7 as a function of $\kappa$ and $b$-purity for the 1991 data. This indicates that the nominal working point selected on a purely statistical basis in Section 4 is indeed close to the minimum for this measurement when systematic effects are taken into consideration. At the nominal $\kappa$ of 0.5 and at a $b$-purity of 88% in the 1992 data, $A_{FB}^{b\bar{b}}$ is measured to be :

$$A_{FB}^{b\bar{b}}\,(1992) \;=\; 11.62 \,\pm\, 1.28\,(stat.) \,\pm\, 0.53\,(syst.) \tag{23}$$

This currently only makes use of the $\delta_b^{widths}$ measurement and corresponds to a $sin^2\theta_w^{eff}$ of :

$$sin^2\theta_w^{eff}\;(1992) \;=\; 0.2285 \,\pm\, 0.0024\,(stat.) \,\pm\, 0.0010\,(syst.) \tag{24}$$

A complete breakdown of the systematic uncertainties on $A_{FB}^{b\bar{b}}$ and $sin^2\theta_w^{eff}$ is given in Table 8. No $\chi$ error is listed here as the $\delta_b$ used does not yet include the lepton analysis which is the only source of such a dependence. The dominant contribution to Table 8 is that from the statistical and systematic errors from $\delta_b^{widths}$ measurement. These are both dependent on the data and

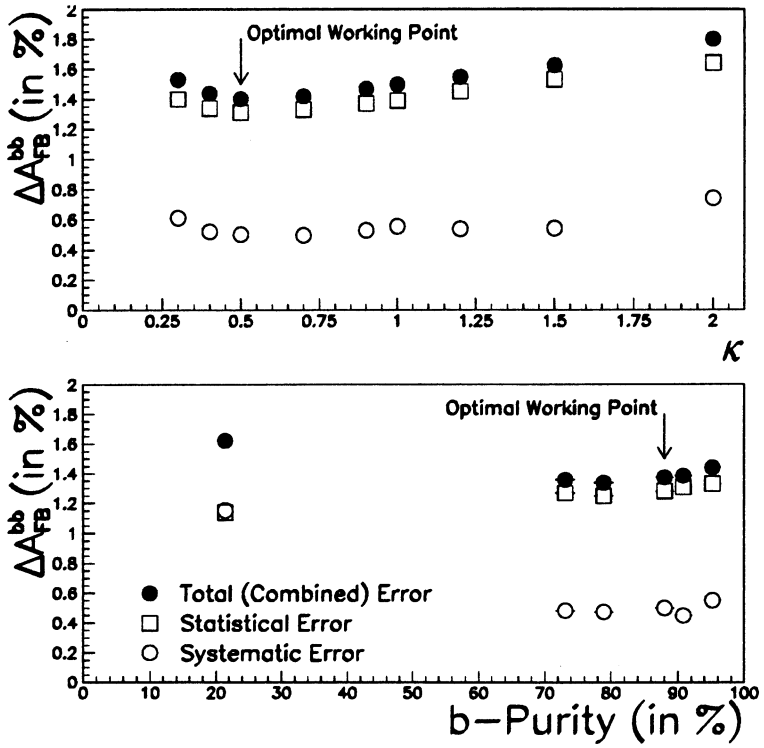


Figure 7: *Summary of the total, statistical and systematic errors on $A_{FB}^{b\bar{b}}$ as a function of the $\kappa$ and b-purity at which it is measured. The optimal values of ($\kappa$,b-purity) at which the measurement is made are also indicated.*

| *Source of Systematic Error* | $\Delta\ A_{FB}^{bb}$ | $\Delta\ sin^2\theta_w^{eff}$ |
|---|---|---|
| *Systematic Error on* $\delta_b$ | 0.38 % | 0.00070 |
| *Statistical Error on* $\delta_b$ | 0.23 % | 0.00042 |
| *Stat. and Syst. Error on Tag Purity* | 0.20 % | 0.00037 |
| *Experimental Systematics on* $\langle Q_{FB}^{btag} \rangle$ | 0.18 % | 0.00035 |
| *Systematic Error on* $\delta_{u,d,s,c}$ | 0.10 % | 0.00019 |
| *Statistical Error on the Acceptance* | 0.05 % | 0.00010 |
| *Systematic Error on the Acceptance* | 0.05 % | 0.00010 |
| *Systematic from* QCD *corrections* | 0.04 % | 0.00008 |
| *Statistical Error on* $\delta_{u,d,s,c}$ | 0.02 % | 0.00004 |
| *Systematic Error from* $\cos\theta$ *Purity Range* | 0.02 % | 0.00004 |
| $\chi$ *Error from* $\delta_b^{lepton}$ | 0.00 % | 0.00000 |
| *Total Systematic Error* | 0.53 % | 0.00010 |

Table 8: *Summary of the systematic errors on $A_{FB}^{b\bar{b}}$ and $sin^2\theta_w^{eff}$ in the 1992 data for the nominal $\kappa$ and b-purity values quoted in the text.*

Monte Carlo statistics used[16] and are significantly reduced when combined with the prospective $\delta_b^{lepton}$ measurement. This means that the $\langle Q_{FB}^{btag} \rangle$ experimental systematics and error on the $b$-purity become the dominant systematic uncertainties on this measurement. As a consequence, it is interesting to study the overall behaviour of the extracted quantities as a function of the

[16]This measurement is currently based upon the 1992 data and Monte Carlo samples.

severity of the lifetime-tag cut. This is shown in Figure 8 where the error bars are corrected for the statistical correlation between measurements and combined with the uncorrelated systematic errors. This shows that the measurements are stable within the statistical and systematic

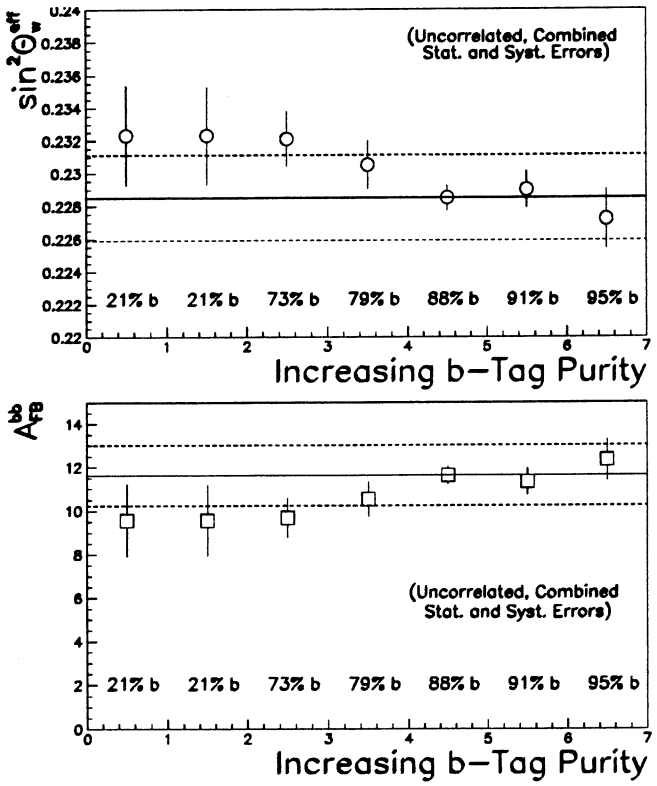


Figure 8: *The extracted physical quantities as a function of increasing lifetime-tag cut and b-purity. The error bars represent the uncorrelated statistical and systematic errors relative to the nominal $\kappa$ of 0.5 and b-purity of 88%. The horizontal bands represent the nominal values and their $\pm 1\sigma$ total error bands.*

uncertainties of the current measurements.

It is possible to repeat the analysis on the 1991 data sample. This represents less than $\frac{1}{3}$ of the size of the 1992 data and so may be expected to lead to a $\sim$ 13% increase of the current precision when they are combined. The 1991 data was taken over a range of energies which must be used in the fitting precedure to correct for the off-peak asymmetries energy-dependence. This is done using ZFITTER to calculate the off-peak values. The extracted value for $A_{FB}^{b\bar{b}}$ in the 1991 data, at the same nominal working point and averaging over all energies, is :

$$A_{FB}^{b\bar{b}}\ (1991) \ = \ 8.13 \ \pm \ 2.10\,(stat.) \ \pm \ 0.53\,(syst.) \tag{25}$$

assuming a systematic error of comparible magnitude. This corresponds to a $sin^2\theta_w^{eff}$ of :

$$sin^2\theta_w^{eff}\ (1991) \ = \ 0.2347 \ \pm \ 0.0039\,(stat.) \ \pm \ 0.0010\,(syst.) \tag{26}$$

The 1991 and 1992 measurements are compatible at the level of $1.4\,\sigma$. However the overall tagging efficiency is 6% lower in 1991 than that found in 1992. To first-order, this has a negligible effect on the purity of the tag but this merits further study when assigning an appropriate systematic error for this data subsample.

Combining the 1991 and 1992 data yields the $A_{FB}^{b\bar{b}}$ value of :

$$A_{FB}^{b\bar{b}}\ (1991 + 1992) \ = \ 10.65 \ \pm \ 1.09\,(stat.) \ \pm \ 0.42\,(syst.) \tag{27}$$

corresponding to a $sin^2\theta_w^{eff}$ of :

$$sin^2\theta_w^{eff}\ (1991+1992) = 0.2303 \pm 0.0020\,(stat.) \pm 0.0008\,(syst.) \tag{28}$$

The *slope* of $\langle Q_{FB}^{btag}\rangle$ versus energy is almost completely independent of $sin^2\theta_w^{eff}$ and depends most strongly on the value of $\delta_b$ found in the data. Using the small amount of off-peak data taken in 1991, the result of the combined 1991 and 1992 fit to $\langle Q_{FB}^{btag}\rangle$ as a function of energy is shown in Figure 9. This shows that the predicted slope from the fitting procedure is in

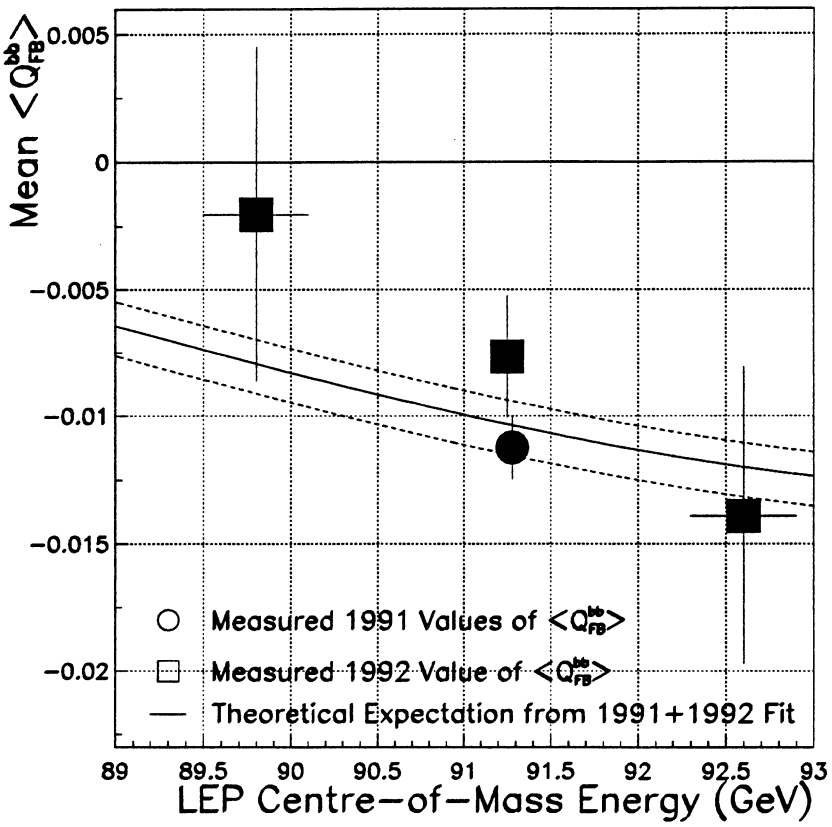


Figure 9: *The energy dependence of the measured asymmetry in the 1991 and 1992 data compared with the fitted theoretical predictions from* ZFITTER *calculations. The lines represent the fitted prediction and its* $\pm 1\sigma$ *bands.*

good agreement with all the 1991 and 1992 data points. The energy dependence is *opposite* to that of the combined quark hadronic asymmetry [2] which is consistent with the removal of the lighter quark flavours from the sample. The prospect of analysing the 1993 data, where large event samples were taken off-peak, is likely to enhance the signifiance of this dependence quite dramatically.

# 11 Conclusions and Prospects

The measurement of $A_{FB}^{b\bar{b}}$ and $sin^2\theta_w^{eff}$ in the 1991 and 1992 data is largely complete and yields a $10\,\sigma$ asymmetry of :

$$A_{FB}^{b\bar{b}}\ \mathbf{(1991+1992)} = \mathbf{10.65 \pm 1.09\,(stat.) \pm 0.42\,(syst.)} \tag{29}$$

with an energy dependence compatible in sign and magnitude with that predicted by the Standard Model and the hemisphere-charge formalism. The leading dependence of the electroweak

corrections on the top quark allows this measurement to determine a $m_t$ value of :

$$m_t = 191 \pm 38 \; GeV/c^2 \;\; (stat.\, only) \tag{30}$$

There are a few remaining areas however where more input is required :

- The updated values of $\delta_b^{lepton}$ will significantly lower the systematic error by reducing both the statistical and systematic uncertainty on the combined $\delta_b$ value. This will also provide a valuable cross-check of the $\delta_b^{widths}$ methodology [12].
- The uncertainty on the lifetime-tag purity in the 1991 data requires further investigation. This is likely to lead to a small increase in the systematic error from this source but with a statistical significance which is relatively small when combined with the 1992 data.

To summarise; the current analysis represents a novel technique for measuring $A_{FB}^{b\bar{b}}$ and $sin^2\theta_w^{eff}$ in ALEPH data where the powerful 3D vertex information of the VDET provides a crucial advantage. The overall precision achieved is roughly comparable to that of the high-$p_T$ lepton analysis [21] but is almost completely statistically independent. The results may then be combined in a simple manner to yield a more powerful measure of the weak mixing angle.

There is also room for further improvements. A new version of the lifetime-tag with an improved efficiency and increased angular coverage is already available [22]. New studies into improving the hemisphere-charge of $b$-quarks are also under way, whilst the $\delta_b^{widths}$ measurement methods can be applied to any new technique to evaluate any new methods in the data itself.

## 12 Acknowledgements

The authors would like to express their thanks to Dave Brown, Alain Blondel, Pascal Perrodo, Rick StDenis and Ingrid ten Have.

## References

[1] The LEP Collaborations; ALEPH, DELPHI, OPAL, L3 and the LEP Electroweak Working Group, *Updated Parameters of the $Z^0$ Resonance from Combined Preliminary Data of the LEP Experiments*, CERN PPE 93-XXX.

[2] D. Decamp et al. (The ALEPH Collaboration), *"Measurement of Charge Asymmetry in Hadronic Z Decays"*, Physics Letters B 259 (1991) 377.

[3] P. Abreu et al. (The DELPHI Collaboration), *"A Measurement of $sin^2\theta_W$ from the Charge Asymmetry of Hadronic Events at the $Z^0$ Peak"*, Physics Letters B 277 (1992) 371.

[4] P.D. Acton et al. (The OPAL Collaboration), *" A Measurement of the Forward-Backward Charge Asymmetry in Hadronic Decays of the $Z^0$"*, Physics Letters B 294 (1992) 436.

[5] A. Falvard et al, *Heavy Flavour Quark Production and Decay Using Prompt Leptons in the ALEPH Detector : Global Lepton Analysis*, ALEPH Note 93-136, PHYSIC 93-117.

[6] D. Abbaneo et al. *$B^0\bar{B}^0$ Mixing and $b\bar{b}$ Asymmetry from High $p_t$ Leptons (Update)*, ALEPH Note 93-109, PHYSIC 93-90.

[7] D. Buskulic et al. (The ALEPH Collaboration), *"A Measurement of $\Gamma_{b\bar{b}}/\Gamma_{had}$ Using a Lifetime b-Tag"*, CERN Preprint PPE 93-108.

[8] D. Brown and M. Frank, *"Tagging b Hadrons Using Track Impact Parameters"*, ALEPH Note 92-135, PHYSIC 92-124.

[9] L. Sawyer (The ALEPH Collaboration), *A Study of the Forward-Backward Charge Asymmetry in Hadronic Z Decays*, Ph.D. Thesis.

[10] A. Halley (The ALEPH Collaboration), *A Study of the Forward-Backward Charge Asymmetry in Hadronic Z Decays*, Ph.D. Thesis, RAL Preprint RALT-120, May 1991.

[11] I. ten Have, *An Updated Measurement of the b Charge Separation in a Lepton-tagged Sample*, ALEPH Note 93-141 PHYSIC 93-121.

[12] A. Halley and P. Colrain, *A Measurement of the b Quark Hemisphere Charge Using a Lifetime-Tag in the 1992 Data*, ALEPH Note 93-161, PHYSIC 93-138.
A. Halley, *Addendum to the Measurement of the b Quark Hemisphere Charge Using a Lifetime-Tag*, ALEPH Note 93-172, PHYSIC 93-147.

[13] D. Buskulic et al. (The ALEPH Collaboration), *"Measurement of $B^0 - \bar{B}^0$ Mixing at the Z using a Jet-Charge Method"*, Physics Letters B 284 (1992) 177.

[14] Private communication with W. Wiedenmann (ALEPH).

[15] I. ten Have, *Comparison of the $\chi$-Dependence of the $A_{FB}^{b\bar{b}}$ Measurement Using High-$p_T$ Leptons or a Jet-Charge Method*, ALEPH Note 93-128, PHYSIC 93-108.

[16] D. Bardin et al, ZFITTER *: An Analytical Program for Fermion Pair Production in $e^+e^-$ Annihilation*, CERN-TH 6443/92, May 1992.

[17] A. Blondel, P. Perrodo, I. ten Have, R. St.Denis, *Update of the Forward/Backward Charge Asymmetry Systematic Errors*, ALEPH Note 93-42, PHYSIC 93-33.

[18] Private communication with Rick StDenis (ALEPH).

[19] A. Halley and P. Colrain, *A Preliminary Measurement of $sin^2\theta_w^{eff}$ from $A_{FB}^{b\bar{b}}$ in the 1992 Lifetime-Tagged heavy Flavour Sample*, ALEPH Note 93-134, PHYSIC 93-115.

[20] A. Halley. Presentation to the Tuesday meeting of the $14^{th}$ December 1993 entitled : *Radiative* QCD *and Resolution Corrections to $A_{FB}^{b\bar{b}}$*

[21] A. Halley and D. Abbaneo, *Prospects for Measuring $A_{FB}^{b\bar{b}}$ and $sin^2\theta_w^{eff}$ at* LEP *I*, ALEPH Note 94-003, PHYSIC 94-003.

[22] Private communication with D. Brown (ALEPH).